Available online at www.sciencedirect.com
ScienceDirect
Journal of Sound and Vibration 303 (2007) 330–342
JOURNAL OF SOUND AND VIBRATION
www.elsevier.com/locate/jsvi

Wind-induced vibration analysis of a cable-stayed bridge during erection by a modified time-domain method

Cheng Su*, Xueming Fan, Tao He

Department of Civil Engineering, South China University of Technology, Guangzhou 510640, PR China

Received 6 May 2006; received in revised form 5 December 2006; accepted 19 January 2007
Available online 21 March 2007

Abstract

In this study, a modified time-domain approach is presented for analytical investigation on the buffeting response of a cable-stayed bridge during erection. Both the frequency-dependent self-excited effects and the imperfect spatial correlation of wind forces over the chord of the bridge deck are taken into consideration in the proposed method. The method represents a modification to the conventional time-domain formulation for the aerodynamic forces directly based on the quasi-steady theory, but remains the advantages of simplicity and straightforwardness as compared with the complicated mixed-formulation in the time-frequency domain. Buffeting responses of the Yamen Bridge at different construction stages, including single pylon stage, maximum double cantilever stage and maximum single cantilever stage, are investigated in this paper by the proposed method. Several conclusions are obtained regarding the above adverse construction stages against wind loads, and the corresponding wind-resistant measures are discussed in the present study.

1. Introduction

The 668 m long Yamen Bridge, as shown in Fig. 1, is a PC cable-stayed bridge with a main span of 338 m and two side spans of 165 m each. It serves as a part of the Western Coastal Highway of Guangdong Province in South China and provides the vital linkage between Zhuhai City and Xinhui City. The bridge deck consists of a PC box girder with a height of 3.48 m and a deck width of 26.8 m for four traffic lanes. The deck is mainly supported by 200 cables approximately 107–136 mm in diameter, which lay in a single plane emanating from the upper parts of the two main towers. The deck is also supported by the main piers, the side piers and also the auxiliary piers between them. Each tower is of a single reinforced concrete pylon that reduces its section area in steps and rises to a level of 128 m. Yamen Bridge is located at the entrance of the South China Sea, crossing the Yamen Channel. The bridge site is mainly affected by tropical cyclones, or typhoons, generally occurring between May and August. It has been recognized that the conditions during bridge erection are often less favorable than those of the final state due to the significant reduction of the overall stiffness of the bridge girder before closing. Therefore, the aerodynamic behavior of the Yamen Bridge during construction is of great concern to the successful completion of the bridge.

*Corresponding author. Tel./fax: +86 20 87110522.
E-mail address: cvchsu@scut.edu.cn (C. Su).

0022-460X/$ - see front matter
doi:10.1016/j.jsv.2007.01.018

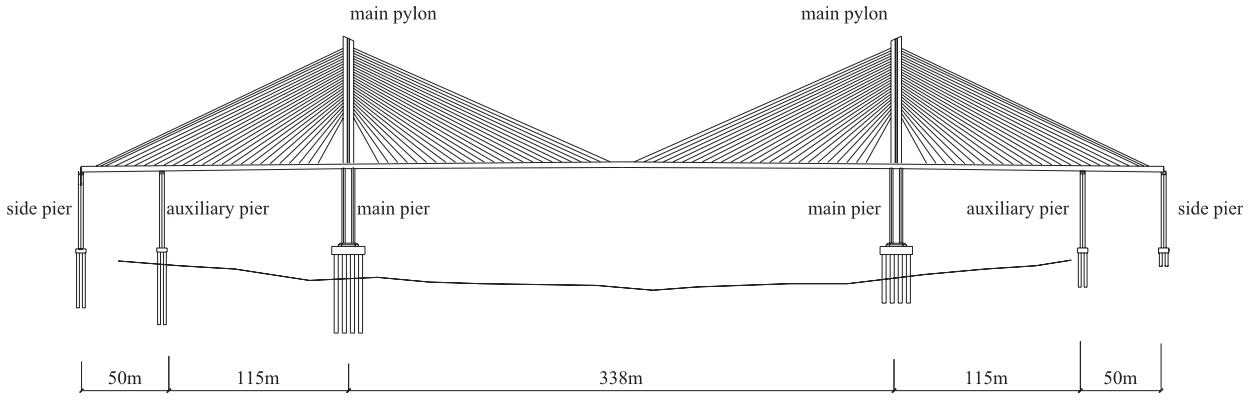

Fig. 1. Elevation of Yamen Bridge.

The dynamic response of a bridge under stochastic wind loads can be studied either in the frequency domain or in the time domain. The conventional frequency-domain analysis with power spectral density functions and coherence functions directly as inputs is based on the linear hypothesis, and hence the total response is obtained by a combination of the contributions from all the vibration modes. This assumption, however, is not appropriate for long-span bridges, where nonlinearity due to either geometric or aeroelastic effects must be considered. As an alternative method, buffeting response of long-span bridges under wind turbulence can be analyzed in the time domain. The method consists of three main steps. First, wind velocity time histories at different locations along the bridge span are artificially generated under certain given power spectral density distributions and coherence functions. Second, the time-domain expressions for the buffeting and self-excited forces acting on the bridge deck are then found from the wind velocities. Third, the equations of motion of the bridge are finally solved by using the step-by-step numerical integration techniques. Among the above steps, the simulation of the aerodynamic forces is the key point that needs careful considerations. Kovacs et al. [1] and Santos et al. [2] put forward a direct time-domain expression for the aerodynamic forces based on the quasi-steady theory, where motion-induced forces are automatically included by using the concepts of relative wind velocity and effective angle of attack. The major advantage of the method lies in its simplicity, since only static coefficients extracted from wind tunnel tests are required in the expression. But there are two issues that need further investigations. First, the self-excited effects in the above method are frequency-independent, which is only valid when low structural reduced frequency fB/U_{m} (or large reduced velocity) prevails, that is, when the time taken for the flow to pass across the bridge deck is short compared with the period of oscillation of the structure [3]. Furthermore, the method implies that the wind forces over the width of the bridge deck are perfectly correlated, based on the assumption that the correlation distance of turbulence is much larger than the size of the deck section [4]. This assumption will deteriorate when higher frequency components are present in the wind turbulence. The above two problems rise from the direct adoption in the aerodynamic force expressions of the static coefficients that are obtained under smooth flow conditions and with the bridge section fixed during wind tunnel tests.

In the current study, a modified time-domain approach is presented for analytical investigation on the buffeting response of the Yamen Bridge during erection. Two sets of frequencies have been considered in the proposed method: those of the structure and those of the wind turbulence. Numerical results are compared with those obtained by full aeroelastic model tests and several conclusions regarding different construction stages are obtained.

2. Simulation of wind fluctuations

For structural design purposes, several models of wind spectra have been proposed. As no reliable measurements of wind spectra are available for the bridge site, the von Karman spectra [1] are recommended for simulation of the wind field for the Yamen Bridge. The partial correlation characteristics of turbulent wind forces over the size of the bridge deck can be taken into account through the use of the frequency-dependent

aerodynamic admittance function, which represents the ratio of fluctuation forces in turbulent flow to quasi-steady forces in smooth flow. In this study, the aerodynamic admittance functions corresponding to the along-wind turbulence and vertical turbulence are respectively expressed as the Davenport and Sears functions [4,5]. To simulate the wind field along the bridge span, the spanwise correlation should be taken into consideration. This may be accomplished by using appropriate spanwise coherence functions. In the present study, the exponential decay expression proposed by Davenport [6] is adopted. The along-wind turbulence u and vertical turbulence w can be considered as stationary Gaussian random processes with zero means and therefore they can be generated using the techniques for digital simulation of multidimensional random processes. An efficient wind field simulation technique for long-span bridges developed by Yang et al. [7] is adopted in this study.

3. Formulation of aerodynamic forces on bridge deck

3.1. Quasi-steady representation of aerodynamic forces

The prerequisite for the aerodynamic analysis of a bridge structure by the time-domain approach is to establish expressions for the fluctuating wind load histories acting on the bridge deck. A natural way to represent the aerodynamic forces is in terms of static force coefficients based on the quasi-steady theory. By considering effects due to deck motions which introduce effective angles of attack and relative wind velocities to the incident wind, the aerodynamic forces at an instant of time, as shown in Fig. 2, are given as

$$F_x(t) = -D(t)\cos\psi + L(t)\sin\psi, \tag{1}$$

$$F_z(t) = D(t)\sin\psi + L(t)\cos\psi, \tag{2}$$

$$M_y(t) = -M(t), \tag{3}$$

where the aerodynamic drag, lift and torque moment in wind axis are expressed as

$$D(t) = \tfrac{1}{2}\rho V_r^2(t) B C_D[\alpha_e(t)], \tag{4}$$

$$L(t) = \tfrac{1}{2}\rho V_r^2(t) B C_L[\alpha_e(t)], \tag{5}$$

$$M(t) = \tfrac{1}{2}\rho V_r^2(t) B^2 C_M[\alpha_e(t)]. \tag{6}$$

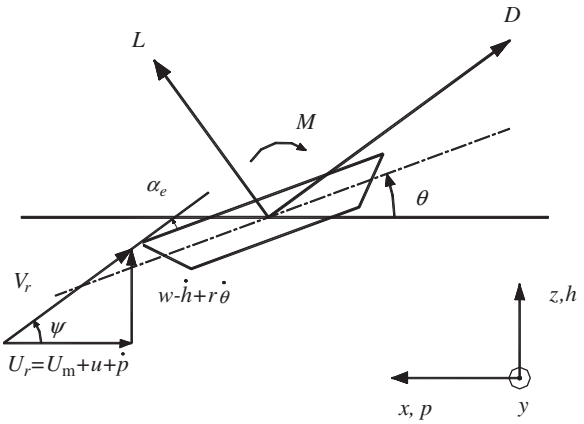

Fig. 2. Effective angle of attack and relative wind velocity.

In Eqs. (4)–(6), $\alpha_e(t)$ and $V_r(t)$ are the effective angle of attack and the relative wind velocity, respectively. They are written as

$$\alpha_e(t) = \psi(t) - \theta(t), \tag{7}$$

$$V_r(t) = \left\{ U_r^2(t) + [w(t) - \dot{h} + r\dot{\theta}]^2 \right\}^{1/2}, \tag{8}$$

where

$$\psi(t) = \left[w(t) - \dot{h} + r\dot{\theta} \right] / U_r(t), \tag{9}$$

$$U_r(t) = U_{\mathrm{m}} + u(t) + \dot{p}. \tag{10}$$

In the above equations, ρ is the air density; B is the deck width; U_{m} is the mean wind velocity at the bridge deck level; $u(t)$ and $w(t)$ are the respective along-wind and vertical fluctuating wind velocities acting on the bridge deck; p, h and θ are the lateral, vertical, and rotation displacements of the bridge deck, respectively; r is assumed to be equal to $B/4$; C_D, C_L and C_M are the respective non-dimensional static coefficients, which can be obtained from wind tunnel test report [8].

3.2. Modification to quasi-steady formulations

In the previous quasi-steady formulations of aerodynamic forces, the static effects due to mean wind velocity, the buffeting effects due to wind turbulence and the self-excited effects due to aeroelasticity are all included at the same time, without being calculated separately and then superimposed. This is true due to the intrinsic nonlinearity of the aerodynamic forces. Furthermore, the dependence of the wind forces on the effective angle of attack is also considered in the formulations. As can be seen, the quasi-steady representation gives a closer and more straightforward interpretation of the physical phenomena of the wind-induced forces.

However, in Eqs. (4)–(6), the force coefficients are only dependent on the effective angle of attack of the incident wind. Actually, frequency domain characteristics of both the wind fluctuation and the bridge deck motion also have effects on the coefficients. It is, therefore, necessary to make certain modifications to the quasi-steady formulations mentioned above. The effect of wind fluctuation frequencies on the coefficients lies in the fact that the wind forces over the chord of the bridge deck are not perfectly correlated. This circumstance may be to some extent compensated by using the aerodynamic admittance functions during wind field simulation, as has been discussed in Section 2. In what follows the dependence of the aerodynamic coefficients on the reduced frequency of the bridge deck oscillation will be addressed.

It has been shown that the values of the incident angles due to the vertical component of wind turbulence, namely, w/U_r in Fig. 2, can vary between $\pm 10^\circ$ [3], while the changes in the incident angles due to deck motions are much smaller. This suggests that drag D, lift L and torque moment M as shown in Eqs. (4)–(6) and $\sin\psi$, $\cos\psi$ in Eqs. (1) and (2) may be given to first approximation by

$$D(t) = \frac{1}{2}\rho V_r^2 B \left(C_{Dw} - K_{Dw}\frac{\dot{h}}{U_r} + K_{Dw}\frac{r\dot{\theta}}{U_r} - K_{Dw}\theta \right), \tag{11}$$

$$L(t) = \frac{1}{2}\rho V_r^2 B \left(C_{Lw} - K_{Lw}\frac{\dot{h}}{U_r} + K_{Lw}\frac{r\dot{\theta}}{U_r} - K_{Lw}\theta \right), \tag{12}$$

$$M(t) = \frac{1}{2}\rho V_r^2 B^2 \left(C_{Mw} - K_{Mw}\frac{\dot{h}}{U_r} + K_{Mw}\frac{r\dot{\theta}}{U_r} - K_{Mw}\theta \right), \tag{13}$$

$$\sin\psi = \sin\psi_w + \cos\psi_w \left(-\frac{\dot{h}}{U_r} + \frac{r\dot{\theta}}{U_r} \right), \tag{14}$$

$$\cos\psi = \cos\psi_w - \sin\psi_w\left(-\frac{\dot{h}}{U_r} + \frac{r\dot{\theta}}{U_r}\right), \tag{15}$$

where

$$\psi_w = w/U_r, \quad C_{Dw} = C_D(\psi_w), \quad C_{Lw} = C_L(\psi_w), \quad C_{Mw} = C_M(\psi_w),$$

$$K_{Dw} = \left.\frac{\mathrm{d}C_D}{\mathrm{d}\alpha}\right|_{\alpha=\psi_w}, \quad K_{Lw} = \left.\frac{\mathrm{d}C_L}{\mathrm{d}\alpha}\right|_{\alpha=\psi_w}, \quad K_{Mw} = \left.\frac{\mathrm{d}C_M}{\mathrm{d}\alpha}\right|_{\alpha=\psi_w}. \tag{16}$$

Substituting Eqs. (11)–(15) into Eqs. (2) and (3) and ignoring small magnitudes of the second order, we have

$$F_z(t) = \frac{1}{2}\rho V_r^2 B\left(C_{Dw}\sin\psi_w + C_{Lw}\cos\psi_w\right) + \frac{1}{2}\rho V_r^2 B\left(H_1\frac{\dot{h}}{U_r} + H_2\frac{B\dot{\theta}}{U_r} + H_3\theta\right), \tag{17}$$

$$M_y(t) = -\frac{1}{2}\rho V_r^2 B^2 C_{Mw} + \frac{1}{2}\rho V_r^2 B^2\left(A_1\frac{\dot{h}}{U_r} + A_2\frac{B\dot{\theta}}{U_r} + A_3\theta\right), \tag{18}$$

where

$$\begin{aligned}
H_1 &= -\left[(K_{Dw} - C_{Lw})\sin\psi_w + (K_{Lw} + C_{Dw})\cos\psi_w\right],\\
H_2 &= \left[(K_{Dw} - C_{Lw})\sin\psi_w + (K_{Lw} + C_{Dw})\cos\psi_w\right]\frac{r}{B},\\
H_3 &= -\left(K_{Dw}\sin\psi_w + K_{Lw}\cos\psi_w\right),\\
A_1 &= K_{Mw}, \quad A_2 = -\frac{K_{Mw}r}{B}, \quad A_3 = K_{Mw}.
\end{aligned} \tag{19}$$

It is well-known that the aerodynamic effects due to $\dot{h}$, $\dot{\theta}$ and θ are related to the reduced frequency of oscillation. Therefore, Eqs. (17) and (18) should be modified by certain corrected coefficients as shown below:

$$\begin{aligned}
F_z(t) = {} & \frac{1}{2}\rho V_r^2 B\left(C_{Dw}\sin\psi_w + C_{Lw}\cos\psi_w\right)\\
& + \frac{1}{2}\rho V_r^2 B\left(h_1H_1\frac{\dot{h}}{U_r} + h_2H_2\frac{B\dot{\theta}}{U_r} + h_3H_3\theta\right),
\end{aligned} \tag{20}$$

$$M_y(t) = -\frac{1}{2}\rho V_r^2 B^2 C_{Mw} + \frac{1}{2}\rho V_r^2 B^2\left(a_1A_1\frac{\dot{h}}{U_r} + a_2A_2\frac{B\dot{\theta}}{U_r} + a_3A_3\theta\right), \tag{21}$$

where h_i and a_i ($i = 1, 2, 3$) are the corrected coefficients related to the reduced frequency (or the reduced wind velocity).

With $p = 0$, $u = w = 0$, and $V_r \doteq U_r = U_m$, the self-excited forces in Eqs. (20) and (21) may be written as

$$F_z^{\mathrm{se}}(t) = \frac{1}{2}\rho U_{\mathrm{m}}^2 B\left[-h_1(K_{L0} + C_{D0})\frac{\dot{h}}{U_{\mathrm{m}}} + h_2(K_{L0} + C_{D0})\frac{r}{B}\frac{B\dot{\theta}}{U_r} - h_3K_{L0}\theta\right], \tag{22}$$

$$M_y^{\mathrm{se}}(t) = \frac{1}{2}\rho U_{\mathrm{m}}^2 B^2\left[a_1K_{M0}\frac{\dot{h}}{U_{\mathrm{m}}} - a_2\frac{K_{M0}r}{B}\frac{B\dot{\theta}}{U_{\mathrm{m}}} + a_3K_{M0}\theta\right], \tag{23}$$

where

$$C_{D0} = C_D(0), \quad K_{L0} = \left.\frac{\mathrm{d}C_L}{\mathrm{d}\alpha}\right|_{\alpha=0}, \quad K_{M0} = \left.\frac{\mathrm{d}C_M}{\mathrm{d}\alpha}\right|_{\alpha=0}. \tag{24}$$

On the other hand, $F_z^{se}(t)$ and $M_y^{se}(t)$ can also be expressed in terms of the aerodynamic derivatives as follows [9]:

$$F_z^{se}(t) = \frac{1}{2}\rho U_m^2 B\left[KH_1^*(K)\frac{\dot{h}}{U_m} + KH_2^*(K)\frac{B\dot{\theta}}{U_m} + K^2H_3^*(K)\theta\right], \tag{25}$$

$$M_y^{se}(t) = \frac{1}{2}\rho U_m^2 B^2\left[KA_1^*(K)\frac{\dot{h}}{U_m} + KA_2^*(K)\frac{B\dot{\theta}}{U_m} + K^2A_3^*(K)\theta\right], \tag{26}$$

where $K = B\omega/U_m$ is the reduced frequency, with ω being the circular frequency of oscillation; H_i^* and A_i^* ($i = 1, 2, 3$) are the aerodynamic derivatives determined by wind tunnel tests [8]. By comparison of Eqs. (22) and (23) with Eqs. (25) and (26), the corrected coefficients can be calibrated as

$$h_1 = -\frac{1}{K_{L0} + C_{D0}}KH_1^*(K), \quad h_2 = \frac{B}{(K_{L0} + C_{D0})r}KH_2^*(K), \quad h_3 = -\frac{1}{K_{L0}}K^2H_3^*(K), \tag{27}$$

$$a_1 = \frac{1}{K_{M0}}KA_1^*(K), \quad a_2 = -\frac{B}{K_{M0}r}KA_2^*(K), \quad a_3 = \frac{1}{K_{M0}}K^2A_3^*(K). \tag{28}$$

It has been observed that bridge structural response is little modified as to mode shapes and frequencies by the influence of the aerodynamic forces due to the dominance of the inertial-elastic forces of the structure relative to the external forces [10]. This suggests that buffeting response to wind turbulence will essentially take place about a few significant natural frequencies corresponding to the major structural mode shapes of the bridge, usually those of the lower orders. Furthermore, for Yamen Bridge, it has been found that the above corrected coefficients do not change significantly versus different vertical or torsional frequencies, especially those corresponding to the direct aerodynamic derivatives. Based on the foregoing observations, the corrected coefficients are thus obtained with respect to the first vertical and torsional frequencies through Eqs. (27) and (28), respectively. Substituting h_i and a_i ($i = 1, 2, 3$) into Eqs. (20) and (21), one can obtain the modified aerodynamic forces for $F_z(t)$ and $M_y(t)$. As for $F_x(t)$, it can be calculated through Eqs. (1), (4) and (5).

4. Buffeting response analysis of Yamen Bridge during erection

Three adverse construction stages against wind loads of the Yamen Bridge, i.e., the single pylon (SP) stage, the maximum double cantilever (MDC) stage and the maximum single cantilever (MSC) stage, are studied in this paper. The SP, MDC and MSC stages refer respectively to the stage just after the completion of the pylon, the stage just before the connection of the side span girder with the auxiliary pier, and the stage just before the closing of the main span. The finite element models for the above three construction stages are shown in Fig. 3. Because the bridge deck is of a PC box girder and mainly supported by stay cables laying in a single plane, the single-girder model without rigid outriggers is adopted for aerodynamic analysis of the bridge. Space beam elements are used to model the bridge girder, the pylon and the piers, with the piers fixed at the bottom ends. In addition, space truss elements are used to represent the stay cables, whose equivalent modulus of elasticity due to sagging is determined by the Ernst's equation [11].

The formulation of wind loading acting on the bridge deck has been established in previous section based on the modified quasi-steady theory. The equivalent static and buffeting forces on the pylons and the piers are estimated by using the corresponding non-dimensional static coefficients recommended by the wind tunnel test report [8], while the self-induced forces on these components are ignored. For cables, only static forces due to mean wind velocity are considered.

On the basis of the above work, analysis of the wind-induced vibration of the bridge at different erection stages and under various mean wind velocities can be carried out by direct integration using the Newmark method. Special attention is paid to the buffeting response of the structures under the design mean wind velocity of 49.7 m/s at the bridge deck level for construction stage. In view of space limitations, only displacement results at selected sections of interest are presented in this paper. In particular, the displacement

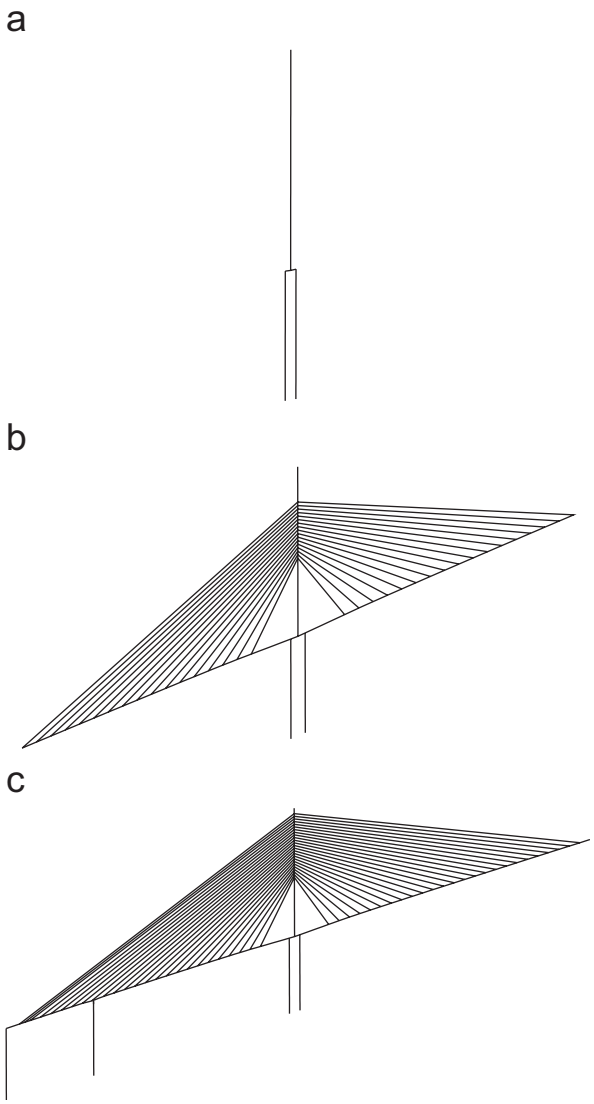

Fig. 3. Finite element models for three adverse construction stages: (a) SP stage, (b) MDC stage, and (c) MSC stage.

time histories are calculated at the top section of the pylon and the cantilever end section of the girder. Fig. 4 shows the time histories of lateral displacement at the top section of the pylon at different construction stages of the bridge. Figs. 5 and 6 show the time histories of displacement components at the cantilever end section of the girder, corresponding to MDC stage and MSC stage respectively. The above displacements are all obtained under the design mean wind velocity of 49.7 m/s, and their statistical values, including the mean displacements, the root mean square (RMS) displacements, the peak displacements and the overall oscillation amplitudes of displacements, are listed in Tables 1–3. The peak values and the overall amplitudes are obtained from the RMS values with the peak factor being taken as 3.5.

It can be seen from Table 1 that the lateral displacement responses of the pylon at SP stage are comparable to those at MDC and MSC stages, while the corresponding axial compression stresses of the pylon due to self-weight at SP stage are much smaller than those at the latter two stages. Under the design mean wind velocity of 49.7 m/s for construction stage, the overall oscillation amplitude of the lateral displacement at the top section of the pylon can reach 350 mm at SP stage, which may induce certain tension stress at the bottom section of the pylon. It is, therefore, necessary to take measures for temporary wind resistance at this stage.

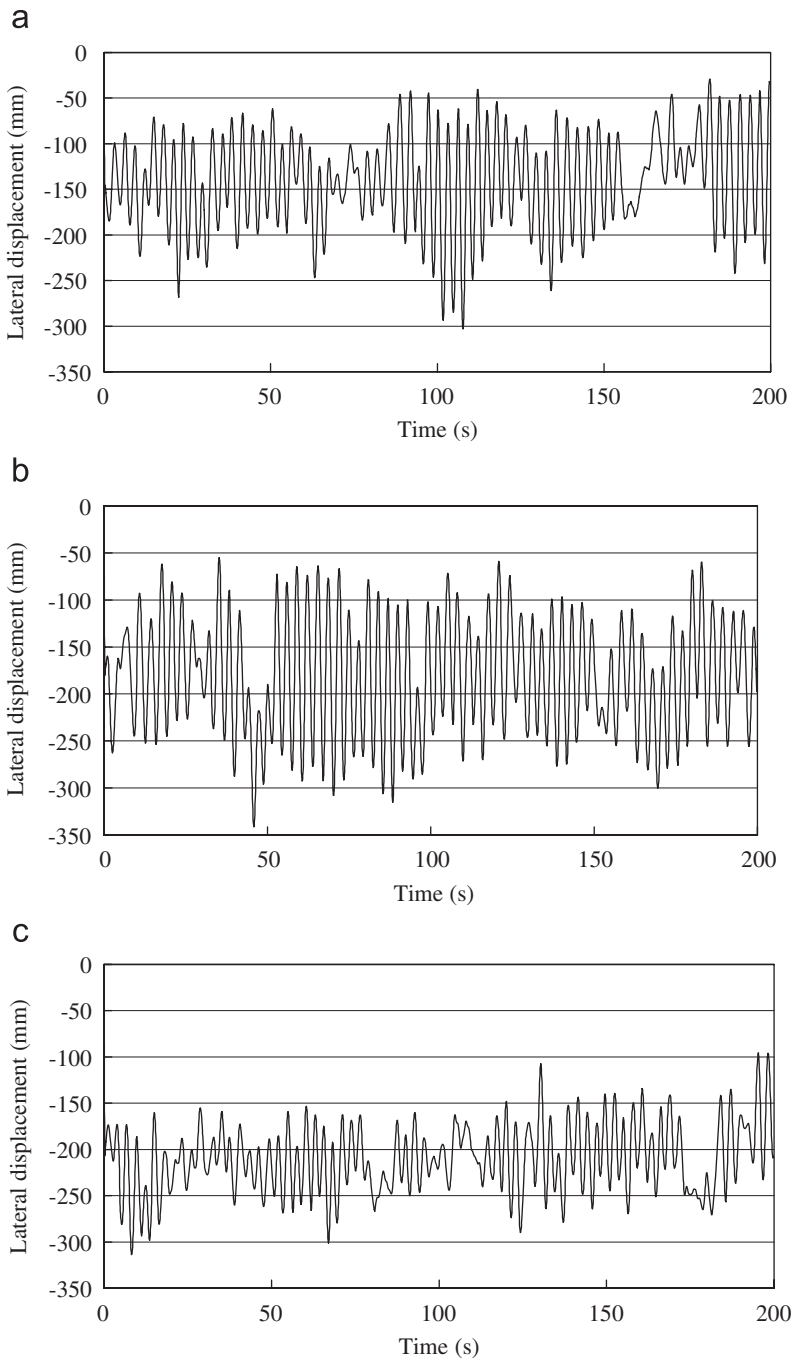

Fig. 4. Time histories of lateral displacement at top section of pylon at different construction stages under $U_m = 49.7$ m/s: (a) SP stage, (b) MDC stage, and (c) MSC stage.

For the Yamen Bridge, two sets of tuned mass damping (TMD) devices were installed at the top of each pylon during this stage, which successfully reduced the vibration amplitude of the pylon by about 50% [12].

Balanced cantilever construction of cable-stayed bridges will result in different structural configurations during erection. When the side span girder reaches above the auxiliary pier, while not connected to it yet, the structure reaches MDC stage with two longest cantilever arms. This stage often has the lowest stiffness and

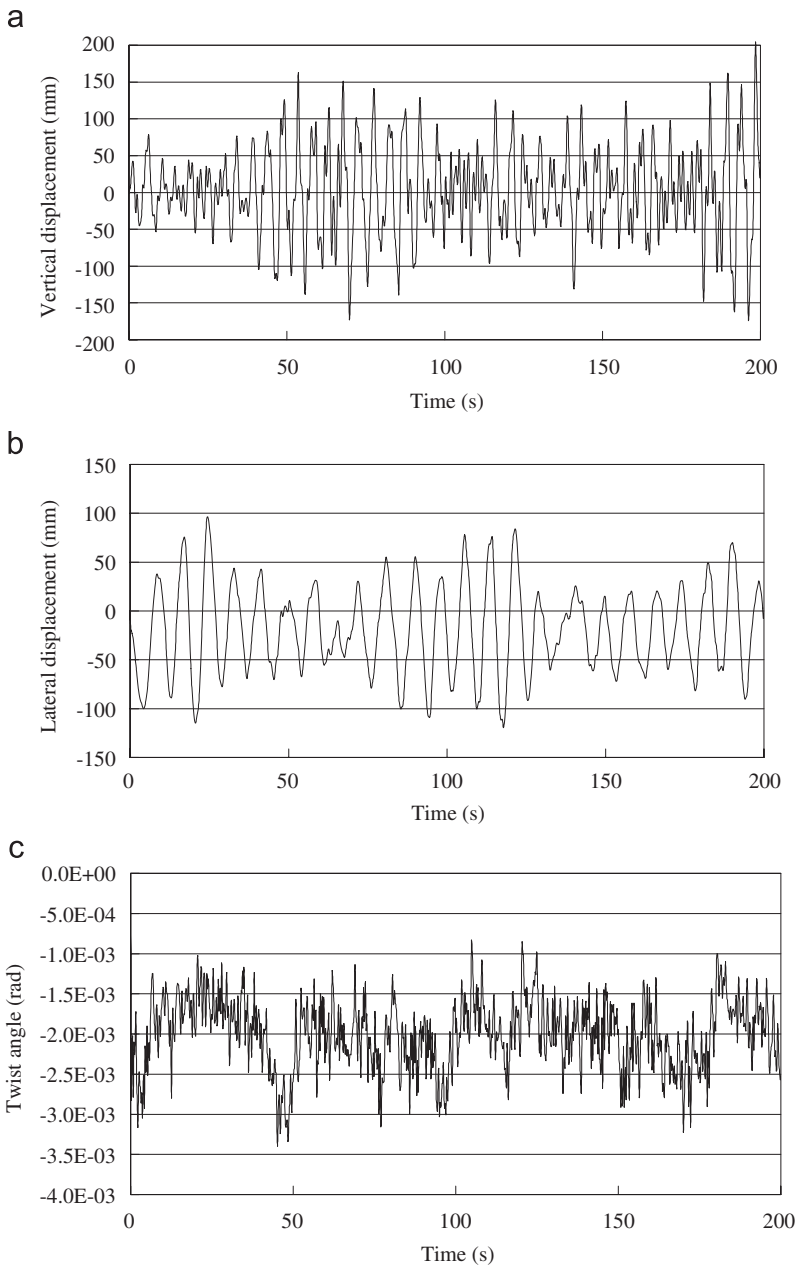

Fig. 5. Time histories of displacement components at cantilever end section of girder at MDC stage under $U_m = 49.7$ m/s: (a) vertical displacement, (b) lateral displacement, and (c) twist angle.

natural frequency, and is more critical in terms of either strength of structural members or aerodynamic instability. For the Yamen Bridge at this stage, the overall oscillation amplitudes of the lateral displacement at the top section of the pylon, the vertical and lateral displacements at the cantilever end section of the girder under $U_m = 49.7$ m/s reach the respective maximum values of 420, 406 and 315 mm, as can be seen from Tables 1–3. Even though the combined response values, including deformations and internal forces, due to both wind turbulence and dead loads under the design mean wind velocity at MDC stage are within the envelope ranges as compared to the design values, large amplitudes of oscillation of the structure will cause difficulties in form level determination and the other geometric measurements during erection. They will also

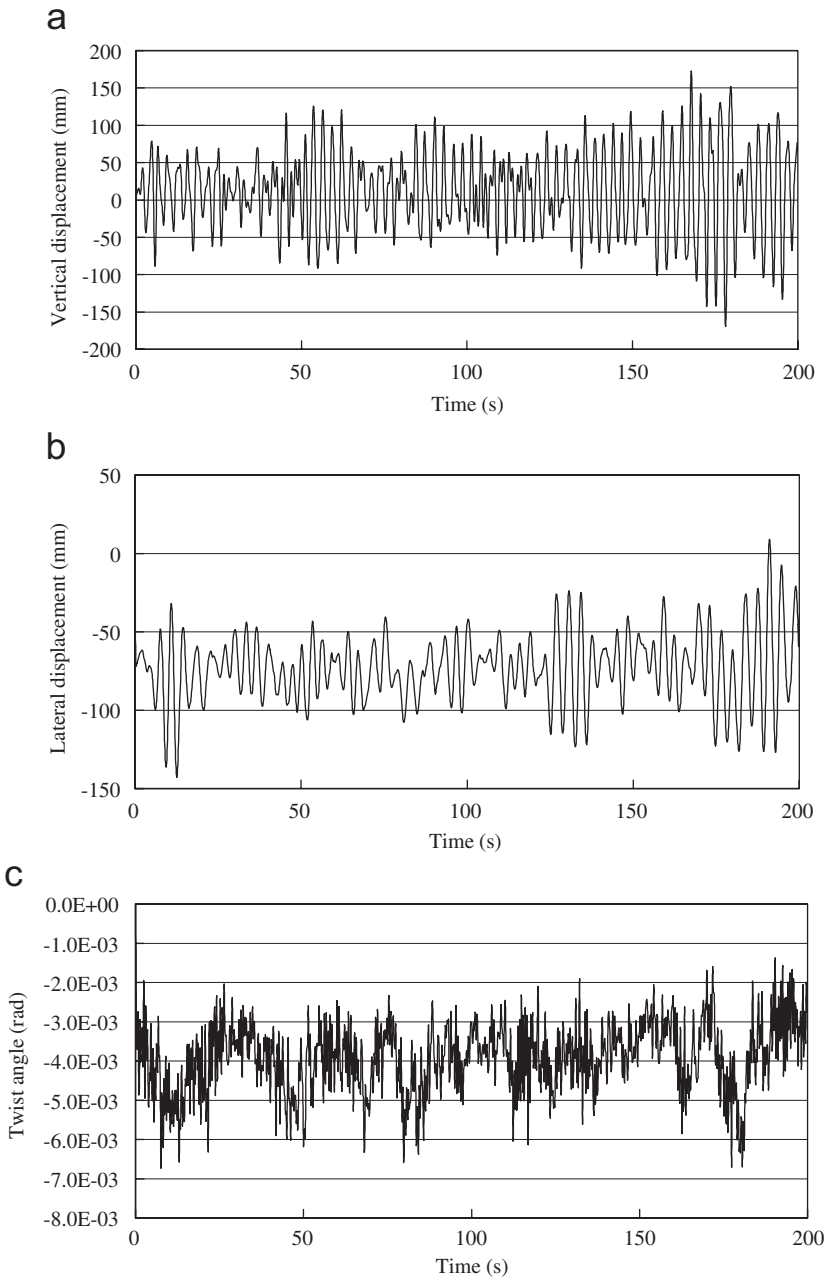

Fig. 6. Time histories of displacement components at cantilever end section of girder at MSC stage under $U_{\mathrm{m}} = 49.7\,\mathrm{m/s}$: (a) vertical displacement, (b) lateral displacement, and (c) twist angle.

Table 1
Statistical results of lateral displacement at top section of pylon under $U_m = 49.7$ m/s.

Construction stage	Mean value (mm)	RMS value (mm)	Peck value (mm)	Overall amplitude of oscillation (mm)
SP stage	−141	50	−316	350
MDC stage	−183	60	−393	420
MSC stage	−210	37	−340	259

Table 2
Statistical results of displacement components at cantilever end section of girder at MDC stage under $U_m = 49.7\,\mathrm{m/s}$

Displacement component	Mean value	RMS value	Peck value	Overall amplitude of oscillation
Vertical displacement (mm)	3	58	206	406
Lateral displacement (mm)	−18	45	−176	315
Twist angle (rad)	−0.00200	0.00045	−0.00358	0.00287

Table 3
Statistical results of displacement components at cantilever end section of girder at MSC stage under $U_m = 49.7\,\mathrm{m/s}$

Displacement component	Mean value	RMS value	Peck value	Overall amplitude of oscillation
Vertical displacement (mm)	11	52	193	364
Lateral displacement (mm)	−73	22	−150	154
Twist angle (rad)	−0.00392	0.00092	−0.00714	0.00560

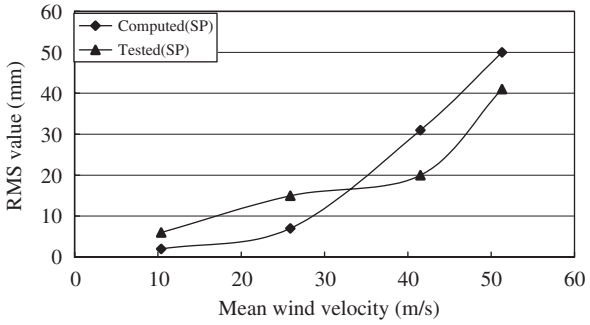

Fig. 7. RMS lateral displacements at top section of pylon at SP stage.

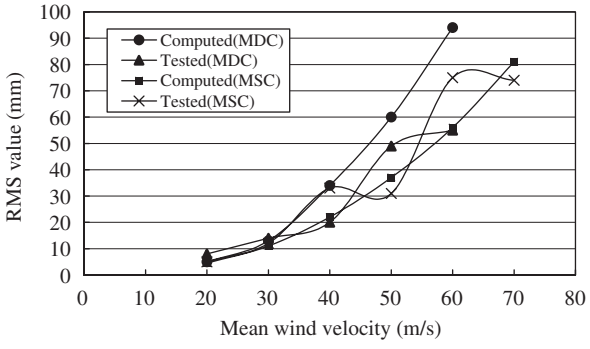

Fig. 8. RMS lateral displacements at top section of pylon at MDC and MSC stages.

lead to the anxiety and upset reactions of the workers working on the bridge deck. The most efficient way to stabilize the structure against buffeting is to increase its fundamental frequency by temporary tie-down cables anchored to pile foundation, dead weights or soil anchors [13]. For the Yamen Bridge, a more simple method was employed to reduce the buffeting response as the side span girder was approaching the auxiliary pier. Temporary connections between the girder and the auxiliary pier were set up by steel frames. After the side

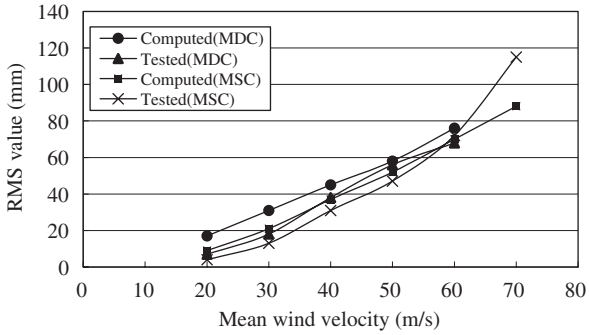

Fig. 9. RMS vertical displacements at cantilever end section of girder at MDC and MSC stages.

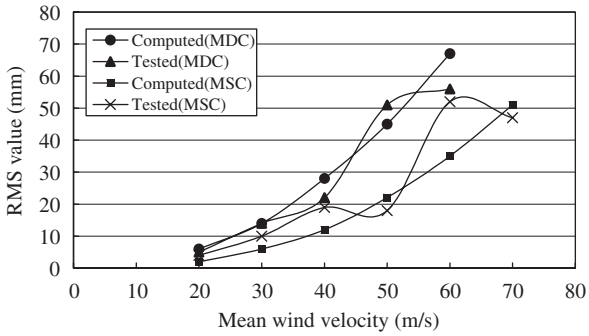

Fig. 10. RMS lateral displacements at cantilever end section of girder at MDC and MSC stages.

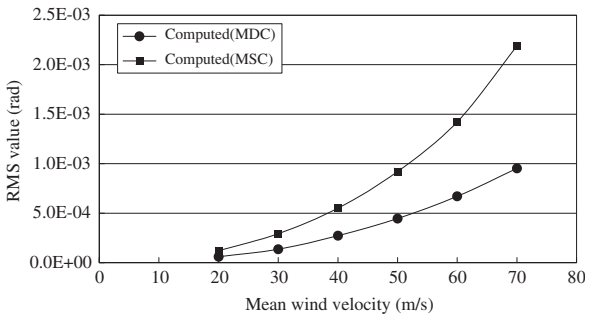

Fig. 11. RMS twist angles at cantilever end section of girder at MDC and MSC stages.

span girder passed over the auxiliary pier, the temporary frames were removed and permanent connections between the girder and the auxiliary pier were eventually built up [12].

To study the aerodynamic behavior of the Yamen Bridge during erection, a series of wind fields corresponding to different mean wind velocities at bridge deck level have been investigated. The RMS lateral displacements at the top section of the pylon at SP stage are given in Fig. 7. For MDC and MSC stages, the RMS lateral displacements at the top section of the pylon, the RMS vertical displacements, lateral displacements and twist angles at the cantilever end section of the girder are illustrated in Figs. 8–11, respectively. No trend of aeroelastic instability of the structure can be identified over the range of wind velocity under study. It can also be seen from Fig. 11 that the twist angles of the girder are relatively small, indicating that the torsional stiffness of the girder is comparatively large. The test results available from wind tunnel test [8] are also given in Figs. 7–10 for comparison. It can be seen in Figs. 9 and 10 that the theoretical

results or tendencies of the RMS displacements of the girder at the cantilever end section are basically in agreement with those obtained from wind tunnel tests. But certain discrepancies between theoretical and test results are observed in Figs. 7 and 8 for the RMS lateral displacements of the pylon at the top section. This could be attributed to various causes, one being the fact that the wind turbulence intensity profile might be more difficult to simulate above the bridge deck level in wind tunnel tests, as has indeed been pointed out in the test report [8]. This may explain why the discrepancies of the RMS lateral displacements at the top section of the pylon appear larger than those at the cantilever end section of the girder. In fact, the experimental results are not that reasonable for some cases. For example, in Fig. 8, the test values for MDC stage are even smaller than those for MSC stage under mean wind velocities of 40 and 60 m/s.

5. Concluding remarks

This paper presents the process of time-domain analysis of structural buffeting responses of the Yamen Bridge during erection under three adverse wind-resistant stages of single pylon, maximum double cantilever and maximum single cantilever, in which the influences of the admittance functions are considered and the conventional quasi-steady formulations for the aerodynamic forces acting on the girder are modified to make them represent the influences of the aerodynamic derivatives of the girder section. Theoretical analysis reveals that the single pylon stage and the maximum double cantilever stage are the respective adverse situations for wind resistance of the pylon and the girder, which was also observed in the wind tunnel tests of full aeroelastic models. The time-domain method proposed in this paper represents a modification to the direct time-domain expression for the aerodynamic forces based on the quasi-steady theory as shown in Refs. [1,2], while remains its simplicity and straightforwardness as compared with the complicated theory employed in Ref. [14], which requires convolution integrals of impulse response functions and nonlinear identification of transfer function constants for calculation of the self-excited effects.

Acknowledgements

This research was conducted in Education Ministry Key Laboratory of Subtropical Architecture, South China University of Technology.

References

[1] I. Kovacs, H.S. Svensson, E. Jordet, Analytical aerodynamic investigation of cable-stayed Helgeland Bridge, *Journal of Structural Division, ASCE* 118 (1) (1992) 147–168.
[2] J.C. Santos, T. Miyata, H. Yamada, Gust response of a long span bridge by the time domain approach, in: K.M. Lam, Y.K. Cheung (Eds.), *Proceedings of Third Asia-Pacific Symposium on Wind Engineering*, Hong Kong, Vol. 1, 1993, pp. 211–216.
[3] G. Diana, S. Bruni, A. Collina, A. Zasso, Aerodynamic challenges in super long span bridges design, in: A. Larsen, S. Esdahl (Eds.), *Bridge Aerodynamics*, Balkema, Rotterdam, 1998, pp. 131–144.
[4] N.P. Jones, R.H. Scanlan, A. Jain, H. Katsuchi, Advances (and challenges) in the prediction of long-span bridge response, in: A. Larsen, S. Esdahl (Eds.), *Bridge Aerodynamics*, Balkema, Rotterdam, 1998, pp. 59–85.
[5] T. Miyata, H. Yamada, V. Boonyapinyo, J. Santos, Analytical investigation on the response of a very long suspension bridge under gust wind, *Proceedings of Ninth International Conference on Wind Engineering*, New Delhi, India, 1995, pp. 1006–1017.
[6] A.G. Davenport, Buffeting of a suspension bridge by storm winds, *Journal of Structural Division, ASCE* 88 (ST3) (1962) 233–268.
[7] W.W. Yang, T.Y.P. Chang, C.C. Chang, An efficient wind field simulation technique for bridges, *Journal of Wind Engineering and Industrial Aerodynamics* 67–68 (1997) 697–708.
[8] Southwest Jiaotong University, Wind Tunnel Report, Report on wind tunnel study on the Yamen Bridge, 1998.
[9] E. Simiu, R.H. Scanlan, *Wind Effects on Structures*, third ed., Wiley, New York, 1996.
[10] R.H. Scanlan, The action of flexible bridges under wind, II: Buffeting theory, *Journal of Sound and Vibration* 60 (2) (1978) 201–211.
[11] J.H. Ernst, Der E-modul von seilen unter berucksichtigung des durchhangs, *Der Bauingenieur* 40 (2) (1965) 52–55.
[12] Guangdong Western Coastal Highway Limited Company, *Yamen Bridge Engineering*, China Communications Press, Beijing, 2004.
[13] W.F. Chen, L. Duan, *Bridge Engineering Handbook*, CRC Press, New York, 2000.
[14] C. Su, D.J. Han, Q.S. Yan, F.T.K. Au, L.G. Tham, P.K.K. Lee, K.M. Lam, K.Y. Wong, Wind-induced vibration analysis of the Hong Kong Ting Kau Bridge, *Structures & Buildings, ICE* 156 (SB3) (2003) 263–272.